JOURNAL OF MAGNETIC RESONANCE **126,** 95–102 (1997)
ARTICLE NO. MN971147

Dynamic Hydrogen Disorder in Solid Tropolone. A Single-Crystal NMR Study of the Hydroxyl Deuterons

A. Detken,* H. Zimmermann,* U. Haeberlen,* and Z. Luz†

*Max-Planck-Institut für Medizinische Forschung, AG Molekülkristalle, Jahnstraße 29, 69120 Heidelberg, Germany; and †Department of Chemical Physics, Weizmann Institute of Science, Rehovot 76100, Israel

Received December 19, 1996

The orientation and temperature dependences of the deuterium NMR spectrum and spin–lattice relaxation time of the hydroxyl deuterons in single crystals of tropolone-d_1 are reported. The results are interpreted in terms of a dynamic hydrogen disorder model in which the hydrogen nuclei move in an asymmetric double well potential. According to this model, the hydrogen-bonded dimer structure as determined by X-ray diffraction constitutes a majority species in the tropolone crystal, comprising more than 98% of the molecules at room temperature. However, there also exists a tautomeric minority species formed by a concerted back and forth shifting of the hydroxyl hydrogens (deuterons) along the hydrogen bonds to the nearby carbonyl oxygens. This process results in a modulation of the electric field gradient tensor at the site of the deuterons, thus providing an efficient relaxation mechanism. The concentration of the minority species is too low and its lifetime is too short to make its direct observation possible. Still, structural information about this species and kinetic and thermodynamic parameters of the hydrogen shift process can be derived by fitting the measured T_1 values to the above model. © 1997 Academic Press

INTRODUCTION

The X-ray structure of the tropolone ($C_7O_2H_6$) shows that the molecules are arranged as centrosymmetric hydrogen-bonded dimers (*1, 2*). The lattice is well ordered and, in particular, no disorder in the position of the hydroxyl hydrogens is observed. The compound crystallizes in the monoclinic space group $P2_1/c$ with two crystallographically related dimers per unit cell, aligned almost parallel to the a^*b^* plane of the reciprocal lattice. The high crystal order is reflected by three facts: a definite peak is observed in the difference synthesis map of the X-ray data that corresponds to the hydrogen atom attached to only one oxygen; the C–O bond length is significantly shorter for one of the oxygen atoms than for the other; and bond length alternation is observed in the seven-membered ring. Each hydroxyl group participates in a bifurcated hydrogen bond with two carbonyl oxygens, one of which belongs to the same molecule, whereas the other is part of the partner molecule in the dimer.

It therefore came as a surprise when Szeverenyi *et al.* (*3, 4*) discovered by MAS ^{13}C 2D-exchange NMR that tautomeric hydrogen shifts between the hydroxyl and carbonyl oxygens take place in crystalline tropolone:

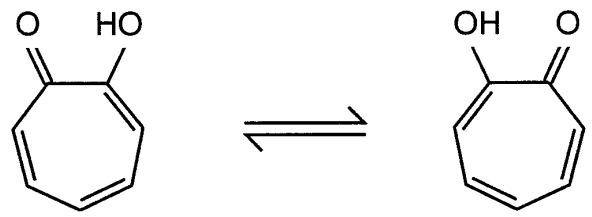

Such a process by itself must lead to hydrogen disorder. To conform with the crystallographic results, the authors proposed that the hydrogen shift proceeds in concert with a π flip of the entire molecule (or dimer), thus preserving the lattice order. Later experiments indicated that the hydrogen shift is, in fact, a secondary reaction that occurs after a self-diffusion jump whenever the carbonyl and hydroxyl oxygens end up inverted in their new lattice sites (*5–7*). The correlation time for these self-diffusion processes is approximately 20 s at room temperature and varies as a function of temperature with an activation energy of about 100 kJ·mol^{-1} (*4*).

On substituting the hydroxyl proton of the tropolone molecule with a deuteron (we will henceforth refer to such a molecule as tropolone-d_1), essentially the same rate constants for the hydrogen shift process are observed (*8*). This lack of isotope effect on the reaction rate confirms the proposed self-diffusion mechanism for the exchange reaction: if its rate was governed by the hydrogen shift process, a significant slowdown would result on deuteration of the system (*9*).

However, preliminary deuteron NMR measurements on a powder sample of tropolone-d_1 (*10*) revealed an unexpectedly short spin–lattice relaxation time of the hydroxyl deuterons, of the order of 30 ms at room temperature. This observation is surprising because from the above considerations the deuterons are expected to be essentially static, the self-diffusion process being too slow to provide for an effi-

1090-7807/97 $25.00
Copyright © 1997 by Academic Press
All rights of reproduction in any form reserved.

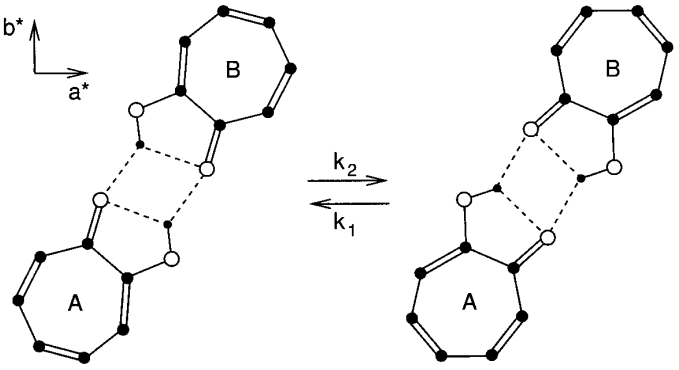

FIG. 1. Projection of the majority (left) and minority (right) species of the tropolone dimer along the crystal axis c. The rate constants of the exchange of the two species are denoted by k_1 and k_2.

cient relaxation mechanism. The main purpose of this paper is to show that this short T_1 of the hydroxyl deuterons reflects the occurrence of another dynamic process in crystalline tropolone that consists of rapid concerted hydrogen shifts within the dimer. The model is similar to that of Benz *et al.* (*11*), who studied the anisotropy of T_1 in single crystals of $KDCO_3$. We present deuteron T_1 measurements in single crystals of tropolone-d_1 as a function of the crystal orientation in the magnetic field and as a function of the temperature. We show that the results can be explained in terms of partial hydrogen disorder involving a majority, long-lived, low-energy species and a minority, short-lived, high-energy species. The model is introduced in the following section, where also a summary of the basic equations necessary to interpret the relaxation results is given. Following Experimental, the relaxation data are presented and analyzed. We conclude with a summary and a comparison with related systems.

THE HYDROGEN DISORDER MODEL

To invoke a relaxation mechanism for the hydroxyl deuterons in tropolone-d_1 in terms of hydrogen disorder, we must assume the presence of at least two interconverting species, the exchange between these providing the mechanism for the relaxation. Specifically, we assume that in addition to the majority dimer structure shown on the left-hand side of Fig. 1, there also exists a less favorable minority structure in which the hydroxyl hydrogens have switched to the neighboring carbonyl oxygens with a concomitant electronic rearrangement in the seven-membered rings, see right-hand side of Fig. 1. In principle, two pathways for the hydrogen shift within the dimer can be imagined, as shown schematically in Fig. 2. In part (a) of this figure, the hydrogen shift from 1 to 2 (1′ to 2′) is *intra*molecular, whereas in part (b) it is *inter*molecular. NMR, however, cannot distinguish between the two alternatives because the inversion symmetry of the dimer renders the two end configurations equivalent.

Both parts (a) and (b) of Fig. 2 imply already the following natural model of the minority species: We assume that the double hydrogen shift process, in concert with the electronic bond rearrangement, results in slight shifts of all the tropolone nuclei in order to restore their equilibrium positions with respect to the new electronic configuration. This assumption seems well justified because the time scale of the concerted hydrogen shift process (see below) is long compared with typical vibrational relaxation rates of the molecule. We further assume that the so-rearranged minority species is congruent with the original majority species, but appears as if flipped by 180° around the line connecting the centers of mass of the two tropolone molecules in the dimer. Part (c) of Fig. 2 illustrates what happens to the O–D bond direction during the hydrogen shift process: the bond direction jumps by 2ϑ, and the model predicts that this angle is 72°. Nevertheless, we will treat 2ϑ as a free parameter which we will determine from the analysis of our T_1 data. In this way, the model will be subjected to an experimental test.

Energetically, the exchange between the majority and minority species can be described by jumps between two in-

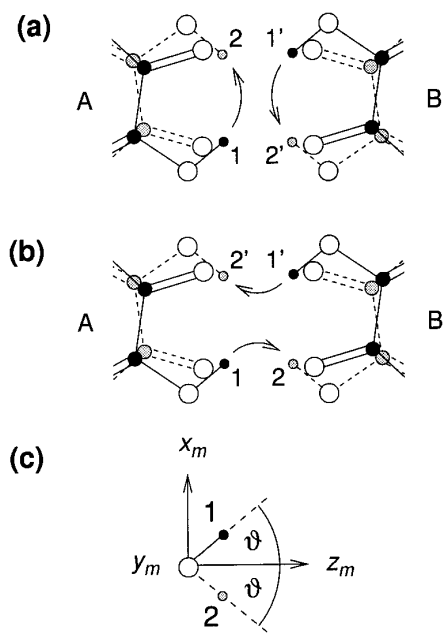

FIG. 2. Superposition of the majority (black circles, full lines) and minority (shaded circles, dashed lines) species of the tropolone dimer. The minority species is drawn according to the model described in the text. In (a), the hydrogen shift is intramolecular, whereas it is intermolecular in (b). Note that NMR cannot distinguish between the two alternatives. (c) illustrates the effect of the hydrogen shift on the direction of the O–D bond and introduces the molecular axes system x_m, y_m, z_m: y_m is perpendicular to the plane of the dimer, and z_m is the bisector of the O–D bond directions in the majority and minority species. A transition from the majority to the minority species, and vice versa, causes the bond angle to jump through an angle of 2ϑ.

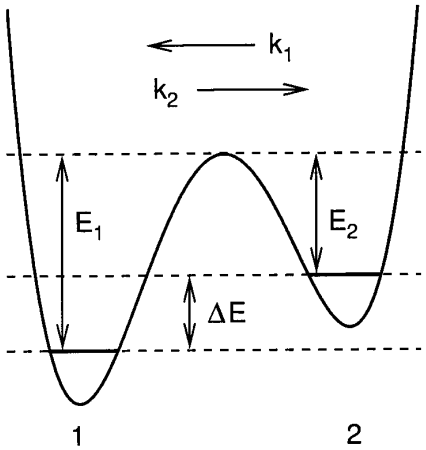

FIG. 3. Sketch of the potential of the tropolone dimer. Minimum 1 corresponds to the nuclear and electronic equilibrium configuration of the majority species, minimum 2 to that of the minority species. The difference between the lowest vibrational levels in the two minima is denoted by ΔE, the distance to the top of the barrier by E_1 and E_2, respectively.

equivalent potential wells with an energy difference ΔE and an average energy barrier $E_a = (E_1 + E_2)/2$, where $E_{1,2} = E_a \pm \Delta E/2$ are the energy differences between the lowest-lying states in the respective potential wells and the top of the barrier, see Fig. 3. A jump between the two sites results in a change of the electric field gradient at the site of the deuteron, thus providing a mechanism for spin–lattice relaxation. Its rate will depend on the electric field gradient (EFG) tensors $\mathbf{V}_1$ and $\mathbf{V}_2$ at the deuteron site in species 1 and 2, respectively, on the fractional populations p_1 and $p_2 = 1 - p_1$ of the two species, and on the correlation time τ_c of the jump process, where

$$\frac{1}{\tau_c} = k_1 + k_2 \qquad [1]$$

is the sum of the forward and backward jump rate constants, see Fig. 3. For such a situation, Benz *et al.* (*11*) gave an expression for T_1^{-1} that reads, when expressed in terms of quadrupole coupling (QC) tensors $\mathbf{Q} = \frac{3}{2}eQ/h \cdot \mathbf{V}$, as follows:

$$\frac{1}{T_1} = \frac{2\pi^2}{9}\left\{\frac{2\tau_c}{1+\omega_0^2\tau_c^2}[(Q_{xz}^{fl})^2 + (Q_{yz}^{fl})^2] + \frac{2\tau_c}{1+4\omega_0^2\tau_c^2}[(Q_{xx}^{fl} - Q_{yy}^{fl})^2 + 4(Q_{xy}^{fl})^2]\right\}. \qquad [2]$$

In Eq. [2], the Q_{ij}^{fl} are the components of a fluctuation quadrupole coupling tensor $\mathbf{Q}^{fl}$ in the laboratory coordinate frame in which z is parallel to the magnetic field $\mathbf{B}_0$. The (time-independent) tensor $\mathbf{Q}^{fl}$ incorporates the effects of the fluctuations of the EFG tensor felt by the deuteron during its hopping process and is given by (*11*)

$$\mathbf{Q}^{fl} = \sqrt{p_1 p_2}\,(\mathbf{Q}_1 - \mathbf{Q}_2). \qquad [3]$$

We assume that $\mathbf{Q}_1$ and $\mathbf{Q}_2$ are congruent (i.e., possess identical principal values), that the perpendicular to the dimer plane is a common principal direction of both $\mathbf{Q}_1$ and $\mathbf{Q}_2$, and that the O–D bond direction in each species is another principal direction (in fact that corresponding to the largest principal component) of $\mathbf{Q}_1$ and $\mathbf{Q}_2$, respectively. In Fig. 2c, we introduce a molecular axes system x_m, y_m, z_m as follows: z_m is the bisector of the O–D bonds of the two species, and y_m is the perpendicular to both these bonds, i.e., the perpendicular to the dimer plane. Note that we know the direction of the O–D bond in the minority species, and therefore the direction of z_m, only within the model described in connection with Fig. 2. Determining this direction experimentally is one of the main goals of this work. In the molecular axes system, the fluctuation tensor acquires the form

$$\mathbf{Q}^{fl} = \sqrt{p_1 p_2}\,\sin 2\vartheta (Q_{ZZ} - Q_{XX}) \begin{bmatrix} 0 & 0 & 1 \\ 0 & 0 & 0 \\ 1 & 0 & 0 \end{bmatrix}, \qquad [4]$$

where 2ϑ is the angle between the O–D bonds in the majority and minority species, respectively, and Q_{ZZ} and Q_{XX} are the in-plane principal components of either $\mathbf{Q}_1$ or $\mathbf{Q}_2$. The fluctuation tensor $\mathbf{Q}^{fl}$ is thus ''flat,'' with a zero principal component along y_m and two other principal components of equal magnitude

$$Q^{fl} = \sqrt{p_1 p_2}\,\sin 2\vartheta (Q_{ZZ} - Q_{XX}) \qquad [5]$$

and opposite signs.[1] The angle between the associated principal axes of $\mathbf{Q}^{fl}$ and x_m, respectively z_m, is $\pm 45°$.

In the molecular axes system x_m, y_m, z_m, Eq. [2] becomes

$$\frac{1}{T_1} = \left(\frac{2\pi}{3}Q^{fl}\right)^2 \left\{\frac{\tau_c}{1+\omega_0^2\tau_c^2}(\cos^2 2\theta_m \cos^2\phi_m + \cos^2\theta_m \sin^2\phi_m) + \frac{\tau_c}{1+4\omega_0^2\tau_c^2} \times (\sin^2 2\theta_m \cos^2\phi_m + 4\sin^2\theta_m \sin^2\phi_m)\right\}, \qquad [6]$$

with θ_m and ϕ_m the polar and azimuthal angles of $\mathbf{B}_0$ in this

[1] In the equations of Ref. (*11*) corresponding to Eqs. [4] and [5], there is an error of a factor of 2. Consequently, the result for p_2 at the temperature (253.7 K) at which T_1 was measured in that paper is too low by a factor of 4. Appropriate corrections must also be applied to the dynamic parameters ΔE and E_a.

axes system. For the case of an axially symmetric QC tensor, Eq. [6] reduces to Eq. [36] of Ref. (*12*). By measuring the orientational dependence of $1/T_1$, we may hope to confirm the proposed dynamic model and to derive kinetic and structural parameters related to the dynamic disorder in the tropolone dimers. Let us therefore briefly discuss the type of behavior we expect for $1/T_1$ for different orientations of $\mathbf{B}_0$. The parameter which influences this dependence most strongly is $\omega_0\tau_c$. If $\omega_0\tau_c \ll 1$, it follows that $1/T_1$ is equal to $(2\pi Q^{fl}/3)^2\tau_c$ when $\mathbf{B}_0$ is in the $x_m z_m$ plane and equal to $(4\pi Q^{fl}/3)^2\tau_c$ when $\mathbf{B}_0$ is along y_m. No anisotropy in T_1 should therefore be observed if the magnetic field scans the plane perpendicular to y_m, while a change by a factor of four in T_1 is expected when $\mathbf{B}_0$ moves in any plane that includes y_m. If, on the other hand, $\omega_0\tau_c \gg 1$, the relaxation rate $1/T_1$ is constant with a value of $(2\pi Q^{fl}/3)^2/(\omega_0^2\tau_c)$ when $\mathbf{B}_0$ moves in the $x_m y_m$ or $y_m z_m$ plane, but anisotropic in the $x_m z_m$ plane with a minimum value of $(\pi Q^{fl}/3)^2/(\omega_0^2\tau_c)$ at $\pm 45°$ from x_m or z_m. Finally, if $\omega_0\tau_c \approx 1$, as happens to be the case in the tropolone-d_1 system at around room temperature, the behavior is more complicated, and special care is required in the analysis of the experimental results.

To derive values for E_a and ΔE, the temperature dependence of T_1 must be measured. We assume that the hydrogen shift process is thermally activated with the correlation time τ_c given by Eq. [1], where the forward and backward jump rate constants $k_{1,2}$ are

$$k_{1,2} = \frac{1}{\tau_0}\exp\left(-\frac{E_{1,2}}{RT}\right). \qquad [7]$$

Also, we assume that the ratio of the populations of the two species is given by the Boltzmann factor

$$\frac{p_2}{p_1} = \exp\left(-\frac{\Delta E}{RT}\right). \qquad [8]$$

According to Eqs. [2] and [3], both τ_c and p_2/p_1 influence the temperature dependence of the relaxation rate. Specifically, assuming $p_2 \ll p_1$ at temperatures where $\omega_0\tau_c \gg 1$, the logarithm of the relaxation rate should be proportional to the inverse absolute temperature with a negative slope of $-(E_a + \frac{1}{2}\Delta E)/R$, whereas for $\omega_0\tau_c \ll 1$ the corresponding slope is $(E_a - \frac{3}{2}\Delta E)/R$, which can be either positive or negative. When $\omega_0\tau_c \approx 1$, the slope will in general change with temperature.

EXPERIMENTAL

Tropolone-d_1 (m.p. 51–52°C) was prepared from the isotopically normal compound by repeated exchange with CH_3OD. After distilling off the remaining methanol, the tropolone-d_1 was purified by sublimation. Single crystals of tropolone-d_1 were grown in a flat, cylindrical vial (diameter 10 cm, height 2.5 cm) evacuated to 10^{-5} torr. The vial was kept under a small (~2 K) temperature gradient at ambient environment. After a few days, seeds appeared on the upper (colder) flat wall. The vial was turned over and the process repeated several times until square shaped crystals of typical dimensions 3 × 3 × 1.5 mm with well–developed growth planes appeared. The flat side of the crystals corresponds to the crystallographic *ac* plane.

The crystals were oriented with an optical two-circle goniometer, glued to a PVC rod, and machined on a lathe to fit into standard 5 mm NMR sample tubes that could be rotated in the NMR probe around an axis perpendicular to the magnetic field $\mathbf{B}_0$. To prevent the crystals from contact with air and humidity, which would lead to loss of deuterium and to rapid deterioration, they were covered with PTFE (Teflon) spray and embedded in epoxy. Even with this precaution, several crystals deteriorated severely in the course of crystal handling and some preliminary experiments.

As the axes of the standard orthogonal system (SOS) in which we carry out all calculations of our data analysis, we choose the crystallographic axes a, b, and c^*. Directions in the SOS will be specified by the polar angles θ and ϕ. Because the crystal is monoclinic and there are two crystallographically related, but magnetically inequivalent sites in the unit cell, a single rotation of the crystal in the magnetic field $\mathbf{B}_0$ around a suitably chosen axis would suffice, in principle, to fully determine any traceless second-rank tensor such as a deuteron quadrupole coupling tensor. Tesche *et al.* (*13*) considered the accuracy of such measurements and proposed choices of the rotation axis for which the measurement errors due to uncertainties in the orientation of this axis are minimized. Nevertheless, we chose two crystals for our measurements on tropolone-d_1. Following the considerations of Tesche *et al.*, one of them was prepared with an angle of ~22° between the monoclinic plane and the rotation axis whose polar angles were chosen as $\theta = 106.5°$ and $\phi = 203.5°$. We refer to this specimen as crystal I. Some additional measurements were performed on a crystal mounted in such a way that the rotation axis coincides with the b axis ($\theta = 90°$, $\phi = 90°$). We refer to this specimen as crystal II. The accuracy of the crystal orientation is estimated to be better than 1°.

Deuteron NMR measurements were performed on a Bruker CXP300 spectrometer operating at 46.07 MHz, using a variable temperature probe equipped with a homemade goniometer for crystal rotation around an axis perpendicular to $\mathbf{B}_0$. Spectra were recorded using the quadrupole echo sequence with a time interval of 20 μs between the pulses. The 90° pulse length was 2.5 μs. Spin–lattice relaxation measurements were performed by inversion recovery using a composite pulse for inversion and a quadrupole echo sequence for detection.

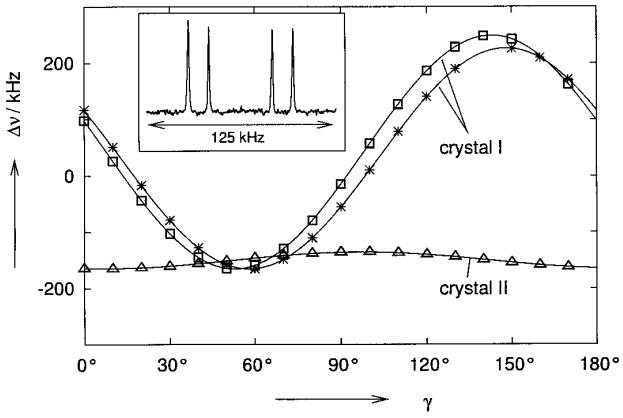

FIG. 4. Rotation pattern of the deuteron NMR doublet splittings $\Delta\nu$ of the crystals I and II of tropolone-d_1 recorded at 294 K. For crystal II, the magnetic field $\mathbf{B}_0$ moves in the monoclinic plane; hence only one doublet is observed. The curves fitted to the experimental data correspond to the deuteron quadrupole coupling tensor $\bar{\mathbf{Q}}$(294 K) in Table 1. The inset shows the spectrum of crystal I for the rotation angle $\gamma = 24°$; acquisition with 200 scans, 500 ms repetition time.

RESULTS AND DISCUSSION

Quadrupole Coupling Tensors

In a general orientation of $\mathbf{B}_0$, the spectrum of a single crystal of tropolone-d_1 consists of two pairs of lines arising from the two symmetry-related, but magnetically inequivalent dimers in the unit cell, see insert in Fig. 4. The lines have a nearly Gaussian shape with full-width at half-maximum height of about 1.2 kHz. For $T = 294$ K, the dependence of the quadrupole splitting $\Delta\nu$ on the rotation angle γ is plotted in Fig. 4 for both crystals I and II. For crystal II, the magnetic field moves in the monoclinic plane; hence both dimers in the unit cell are magnetically equivalent, and only one doublet is observed. Because the O–D bonds of the majority species are approximately parallel to the *b* axis (*1*), the observed splittings for this crystal are almost independent of the rotation angle γ. The origin of the angle γ is defined (arbitrarily) in such a way that at $\gamma = 21.2°$ the magnetic field $\mathbf{B}_0$ is parallel to the c^* axis. For crystal I, two doublets are observed in most orientations. Here, $\gamma = 55.4°$ corresponds to the rotation angle where $\mathbf{B}_0$ crosses the monoclinic plane. This occurs at $\theta = 17.8°$, $\phi = 180°$. Similar measurements were performed at 236 K. The deuteron quadrupole coupling tensors $\bar{\mathbf{Q}}$(294 K) and $\bar{\mathbf{Q}}$(236 K) derived from the data at both temperatures are listed in Table 1. The principal axes are given for that dimer which is denoted A–B by Shimanouchi and Sasada (*2*). In Fig. 4, the splittings of this dimer observed in crystal I are marked with squares. The polar angles of the principal axes for the other dimer can be obtained through the monoclinic symmetry by replacing $\theta \rightarrow 180° - \theta$, $\phi \rightarrow 180° - \phi$. The assignment of the coupling tensors to the corresponding dimers is based on the assumption that the principal directions e_Z lie *in* the dimer plane. In practice, for one of the possible assignments these directions were found to lie in the dimer planes as determined by X-rays within less than 1°, while the reverse assignment would place them 5° off these planes.

We note that there is only a very slight change in the magnitude of the principal components of the QC tensor on decreasing the temperature from 294 to 236 K and that there is no significant effect on the orientation of the principal directions. The high accuracy in the determination of the QC tensors is demonstrated by the fact that, despite the smallness of the asymmetry parameter η, essentially the same orientations were found for the principal directions $\mathbf{e}_X$ and $\mathbf{e}_Y$ at both temperatures. In both cases, the principal direction $\mathbf{e}_Y$ is nearly perpendicular to the dimer plane, as is expected from the local symmetry of the system.

Anisotropy of T_1

The orientation dependence of $1/T_1$ for crystal I was measured at two temperatures, 294 and 267 K. The results for the two dimers in the unit cell are plotted in Fig. 5, using the same symbols as in Fig. 4. The data exhibit a pronounced anisotropy with almost a factor of four between the minimum and maximum values.

We first discuss the room temperature results. As explained in the previous section, we require that the fluctuation tensor $\mathbf{Q}^{\mathrm{fl}}$ be ''flat,'' i.e., traceless with one principal component being zero and the two others having values $\pm Q^{\mathrm{fl}}$. Furthermore, the principal direction with the zero prin-

TABLE 1
The Various Quadrupole Coupling Tensors of the Hydroxyl Deuterons in Tropolone-d_1

Tensor	Principal component	Principal value (kHz)	Principal direction[a] θ	Principal direction[a] ϕ
$\bar{\mathbf{Q}}$ (294 K)	*ZZ*	301.9	88.3°	92.7°
(η = 0.097)	*YY*	−165.6	164.5°	8.7°
	XX	−136.3	74.6°	2.2°
$\bar{\mathbf{Q}}$ (236 K) ($\approx\mathbf{Q}_1$)	*ZZ*	311.2	88.6°	92.9°
(η = 0.078)	*YY*	−167.7	164.0°	8.0°
	XX	−143.5	74.0°	2.5°
$\mathbf{Q}_2$	*ZZ*	311.2	75.8°	18.1°
	YY	−167.7	165.3°	2.9°
	XX	−143.5	86.3°	287.2°
$\mathbf{Q}^{\mathrm{fl}}$ (294 K)	*ZZ*	54	90°	100°
	XX	−54	75°	10°

[a] The angles θ and ϕ denote polar angles in the standard orthogonal system with axes parallel to *a*, *b*, and c^*. Principal directions are given for the dimer denoted A–B by Shimanouchi and Sasada (*2*). The symbol η denotes the asymmetry parameter defined as $\eta = (Q_{XX} - Q_{YY})/Q_{ZZ}$.

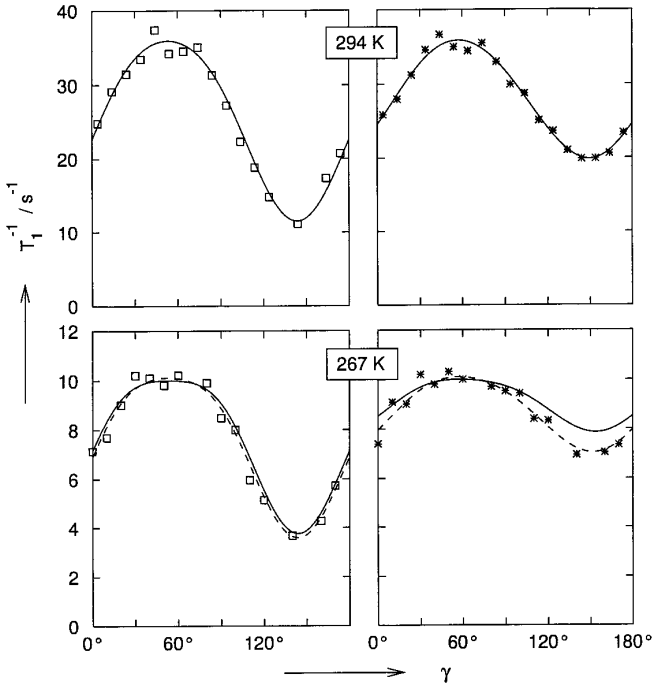

FIG. 5. Rotation patterns of the spin–lattice relaxation rates $1/T_1$ of the two magnetically distinct deuterons in the crystal I of tropolone-d_1, recorded at $T = 294$ K and $T = 267$ K. Open squares correspond to the dimer A–B in the notation of Ref. (*2*), asterisks to the glide symmetry-related dimer. The full curves in the 294 K patterns are fits to Eq. [6]. In the 267 K patterns, the full (dashed) curves were calculated with the fluctuation tensor extracted from the 294 K data and the thermodynamic parameters extracted from the temperature dependence of $1/T_1$ shown in Fig. 6, without (with) invoking an entropy term.

cipal component should be perpendicular to the dimer plane ($\theta = 165.5°$, $\phi = 9.0°$). Using these restrictions, Eq. [6] was fitted to the experimental data in Fig. 5 with Q^{fl}, $\omega_0\tau_c$ and the direction of z_{m} in the plane of the dimer (one additional parameter) being the fitting parameters. The full lines in the upper part of Fig. 5 were obtained by this procedure. The good fit of the experimental data with just three adjustable parameters lends strong support to the underlying assumptions, specifically the assumed orthogonality of y_{m}, the direction corresponding to the zero principal component, to the dimer plane. We find $\omega_0\tau_{\mathrm{c}}(294\ \mathrm{K}) = 1.0$, $Q^{\mathrm{fl}} = 54$ kHz and $\theta = 80.0°$, $\phi = 55.9°$ for the direction of z_{m}. The principal directions of $\mathbf{Q}^{\mathrm{fl}}$ (that are at angles of $\pm 45°$ from z_{m} within the dimer plane) are also given in Table 1.

In Fig. 2c, we introduced the angle ϑ as the angle between the z_{m} axis and the O–D bond direction in the majority species. Identifying this latter direction with the principal direction $\mathbf{e}_Z$ of $\bar{\mathbf{Q}}$ at 236 K, we find $\vartheta = 37.5°$, yielding a total jump angle 2ϑ of 75°. From this, we find the O–D bond direction in the minority species to have the polar angles $\theta = 75.8°$ and $\phi = 18.1°$. The result for 2ϑ compares favorably with the prediction from the model introduced in connection with Fig. 2, from which a value of $2\vartheta = 72°$ is expected. In this model, slight shift motions also of the heavy nuclei in the tropolone molecule were assumed as a result of the electronic rearrangement caused by the hydrogen shift process. The good agreement of the predicted and measured values of 2ϑ provides strong evidence for such motions of all atoms in the tropolone molecule.

Thermodynamic Parameters for the Equilibrium and for the Exchange of the Two Species

Now that $\mathbf{Q}^{\mathrm{fl}}$ and ϑ are known, we can use Eq. [4] to calculate the value of $\sqrt{p_1 p_2}$, or, equivalently, the ratio of the occupation probabilities p_2/p_1. We find $p_2/p_1 = 1.56 \times 10^{-2}$ at 294 K, from which number we obtain $\Delta E = -RT \ln(p_2/p_1) = 10.2\ \mathrm{kJ \cdot mol^{-1}}$ for the asymmetry of the double well potential. To obtain the average activation energy E_{a} of the jump process, we must take into account the temperature dependence of $1/T_1$. We measured this dependence for one fixed orientation of the crystal, given by $\gamma = 74°$ in Fig. 5 which corresponds to $\mathbf{B}_0$ having the orientation $\theta = 35.2°$, $\phi = 138.2°$ in the SOS. The results are shown in Fig. 6. Assuming that the temperature dependence of τ_{c} is given by Eqs. [1] and [7], we fitted Eq. [6] to the data of Fig. 6 with the fitting parameters now being just τ_0 and E_{a}. The result of this procedure is the solid line in Fig. 6. The thermodynamic parameters obtained in this way are given in the first row of Table 2.

We now turn to the orientation dependence of $1/T_1$ at 267 K, see lower part of Fig. 5. From the above, we should be able to simulate these results with no additional parameters. The solid line in the lower part of Fig. 5 was indeed calculated using only the parameters obtained so far. The fit is

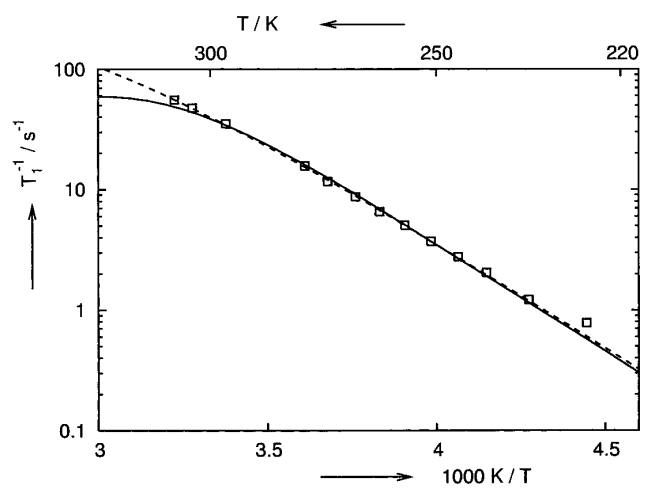

FIG. 6. Temperature dependence of the spin–lattice relaxation rate $1/T_1$ of the deuterons in the A–B dimer of crystal I for the rotation angle $\gamma = 74°$. The full (dashed) curves are fits to Eqs. [6], [7], and [8] (respectively [9]), i.e., without (with) invoking an entropy term.

TABLE 2
Kinetic and Thermodynamic Parameters for the Concerted Deuteron Shifts in Solid Tropolone-d_1

	$1/\tau_0$ (s^{-1})	E_a ($kJ \cdot mol^{-1}$)	ΔE ($kJ \cdot mol^{-1}$)	$\Delta S/R$
No entropy term[a]	5.0×10^{12}	29.0	10.2	—
With entropy term	3.8×10^{10}	23.0	22.2	4.9

[a] See text.

quite reasonable and reproduces faithfully not only the general angular dependence of $1/T_1$, but also, for most orientations, the actual values to within a few percent. It appears, however, that the ratio between the maximum and the minimum values of $1/T_1$ as a function of the crystal orientation is slightly smaller for the calculated curve than for the experimental values. The fit can be improved considerably by introducing an entropy factor to the equilibrium population ratio,

$$\frac{p_2}{p_1} = \exp\left(-\frac{\Delta E}{RT}\right)\exp\left(\frac{\Delta S}{R}\right). \qquad [9]$$

When this relation is used and the overall analysis of the data is repeated, taking ΔS as an additional independent parameter, the results shown in the second row of Table 2 are obtained. The dashed lines in Figs. 5 and 6 were calculated using these parameters. They show a small, but definite improvement of the fit both for the orientation dependence of $1/T_1$ at 267 K and for the temperature dependence of $1/T_1$. Note that by introducing the entropy term, the values for both E_a and ΔE change significantly, making an error estimation for these parameters questionable. We feel that this problem is by no means unique to tropolone. The result for ΔS ($4.9R$) may reflect the disorder and hence higher entropy induced in the crystal by the formation of the minority species in an otherwise well-ordered environment.

So far, we have assumed for the analysis of the relaxation data that $\mathbf{Q}_1$ equals the measured value of the average QC tensor $\bar{\mathbf{Q}}$ at 236 K. From the thermodynamic data in Table 2, the fractional population of the minority site, p_2, is estimated to be 0.5% at 236 K for the parameters without the entropy term and 0.16% for those with the entropy term. Recalling that the measured value of $\bar{\mathbf{Q}}$ is the weighted average of the two species, $\bar{\mathbf{Q}} = p_1\mathbf{Q}_1 + p_2\mathbf{Q}_2$, it is clear that the approximation made is indeed valid.

According to Eq. [7] and the parameters in Table 2, the lifetime of the minority species is 1.1×10^{-8} s at $T = 236$ K (entropy term taken into account). It is even shorter at $T > 236$ K. This short lifetime of the minority species at 236 K and above prevents the direct NMR observation of this species in this temperature range. Although cooling will increase this lifetime, it will also reduce p_2, rendering it highly unlikely that the NMR signal of the minority species can be seen at any temperature.

SUMMARY AND CONCLUSIONS

We have shown that the short relaxation time of the hydroxyl deuterons in crystals of tropolone-d_1 can be quantitatively accounted for in terms of dynamic hydrogen disorder within the dimer units that constitute the building blocks of the lattice. The disorder is brought about by a concerted double hydrogen shift within the dimer, resulting in a minority species which is not well accommodated in the lattice of the majority species. It is therefore short lived and rapidly reverts to the ground state species. The process is accompanied by slight displacements of all atoms of the tropolone molecules which may be responsible for the thermal reorientational motion observed in the X-ray studies (*1, 2*). The occurrence of a minority species may correlate with the high vapor pressure of tropolone and its low melting point of ~50°C, at which temperature the concentration of the minority species is estimated to be about 2%.

Our results complement the earlier dynamic studies of solid tropolone, where the slow exchange process detected in 2D ^{13}C experiments was attributed to self-diffusion. This process is associated with a much higher activation energy and is orders of magnitude slower than the concerted hydrogen shifts investigated in the present work. A self-diffusion step will also be accompanied by a concerted hydrogen shift whenever the molecule ends up with a ''wrong'' position of the carbonyl and hydroxyl oxygens, but the concerted hydrogen shift is not the rate-determining step in this process.

It is interesting to compare the results for the hydrogen dynamics in the tropolone dimer with that occurring in solid carboxylic acid dimers. Scheubel *et al.* (*14*) investigated the hydrogen dynamic disorder in dimethylmalonic acid (DMMA) and summarized results for the activation energy E_a obtained in a number of other carboxylic acid dimers (a total of 16). They showed that the list can be divided into two groups depending on whether E_a is ''small'' (6 ± 3 $kJ \cdot mol^{-1}$) or ''large'' (60 ± 6 $kJ \cdot mol^{-1}$) and argued that in the first group the compound undergoes a simple concerted hydrogen shift in an asymmetric double well potential, whereas in the second group the process most likely (and *certainly* in DMMA) involves a flip of the whole dimeric unit followed by a rapid hydrogen shift. In tropolone, both types of processes take place. The slow tautomeric hydrogen shifts studied by the ^{13}C magnetization transfer techniques (*3–7*) belong to the second class of reaction in which a slow diffusional jump (or flip) is followed by a rapid hydrogen shift. The fact that motions of whole molecules are involved is reflected in the high activation energy (~100 $kJ \cdot mol^{-1}$) associated with these jumps in tropolone (*4*). In

the present work, we studied fast concerted hydrogen shifts within an asymmetric double well potential. The activation energy found for this process ($\sim$25 kJ $\cdot$ mol^{-1}) is considerably lower than for the self-diffusional jumps, but still significantly higher than the typical value of 6 kJ $\cdot$ mol^{-1} found in the dicarboxylic acid dimers for this type of process. The reason might be found in the fact that in the dicarboxylic acid dimers, the electronic bond rearrangement caused by the hydrogen shifts and the associated atomic displacements are essentially restricted to the carboxyl groups, whereas in tropolone all the heavy atoms of the molecule are forced to shift their positions in the course of the hydrogen shift process.

ACKNOWLEDGMENTS

We are grateful to P. Gutsche for his help in orienting, coating, and mounting some of the single-crystal samples and to Z. Olender for making her relaxation data of a powder sample of tropolone-d_1 available to us. These data actually stimulated this single-crystal investigation. This work was supported by a grant from the German–Israeli Foundation for Scientific Research and Development (GIF). One of us (Z.L.) thanks the Humboldt Foundation for a Humboldt Research Award.

REFERENCES

1. H. Shimanouchi and Y. Sasada, *Tetrahedr. Lett.* **28,** 2421 (1970).
2. H. Shimanouchi and Y. Sasada, *Acta Crystallogr. B* **29,** 81 (1973).
3. N. M. Szeverenyi, M. J. Sullivan, and G. E. Maciel, *J. Magn. Reson.* **47,** 462 (1982).
4. N. M. Szeverenyi, A. Bax, and G. E. Maciel, *J. Am. Chem. Soc.* **105,** 2579 (1983).
5. J. J. Titman, Z. Luz, and H. W. Spiess, *J. Am. Chem. Soc.* **114,** 3756 (1992).
6. R. G. Larsen, Y. K. Lee, J. O. Yang, Z. Luz, H. Zimmermann, and A. Pines, *J. Chem. Phys.* **103,** 9844 (1995).
7. Z. Olender, D. Reichert, A. Müller, H. Zimmermann, R. Poupko, and Z. Luz, *J. Magn. Reson.* **120,** 31 (1996).
8. Z. Olender, Ph.D. Thesis, Weizmann Institute of Science, Rehovot, Israel, 1996.
9. H. H. Limbach, *in* ''NMR Basic Principles and Progress,'' Vol. 23, p. 63, Springer-Verlag, Berlin, 1990.
10. Z. Olender, private communication.
11. S. Benz, U. Haeberlen, and J. Tegenfeldt, *J. Magn. Reson.* **66,** 125 (1986).
12. D. A. Torchia and A. Szabo, *J. Magn. Reson.* **49,** 107 (1982).
13. B. Tesche, H. Zimmermann, R. Poupko, and U. Haeberlen, *J. Magn. Reson. A* **104,** 68 (1993).
14. W. Scheubel, H. Zimmermann, and U. Haeberlen, *J. Magn. Reson.* **80,** 401 (1988).